RSC Advances

ROYAL SOCIETY OF CHEMISTRY

www.rsc.org/advances

Journal Name

ARTICLE

Nanoparticles of Pt loaded on vertically aligned TiO_2 nanotube bed: Synthesis and evaluation of electrocatalytic activity

Received 00th January 20xx,
Accepted 00th January 20xx

DOI: 10.1039/x0xx00000x

www.rsc.org/

K. R. Rasmi, S.C. Vanithakumari, R.P. George, C. Mallika and U. Kamachi Mudali*

A well distributed and uniformly covered Pt nano particles loaded TiO_2 nanotube (TiNT) electrode was synthesized via seed mediated hydrothermal reduction method on self aligned TiNT bed obtained using electrochemical anodization of Ti foil in an organic electrolyte. The absence of seeding step resulted in agglomeration of Pt nanoparticles on TiO_2 nanotubes. Surface morphology and Pt nano particle loading were investigated using field emission scanning electron microscope (FESEM) and X-ray energy dispersion spectroscopy (EDS). The phase and chemical state of the synthesized electrode was examined by X-ray diffraction (XRD) and X-ray photoelectron spectroscopy (XPS). The electronic interaction between Pt nanoparticle and TiNT was also established using XPS study. The electrochemical activity of the as-synthesized electrode was estimated for the electrooxidation of methanol and was compared with that for Pt nanoparticle coated on Ti substrate and agglomerated Pt particle coated TiNT. The corresponding results of this study confirmed that the Pt nanoparticle- substrate interaction and size of nanoparticles have a definite role in enhancing the electrocatalytic activity.

Introduction

Nano particles of metals find potential applications in different functional areas such as catalysis, electronics, semi-conductors, sensors, magnetic devices etc. [1-4] owing to their unique size related structural and chemical properties like high specific surface area and quantized electronic structure [5]. Among them, nanomaterials based on Pt have been subjected to extensive research as it is an excellent catalyst material in many energy related fields [4]. The excellent corrosion resistance along with electrical conductivity offered by Pt makes it the best candidate material as electrodes for various industrial applications [6-12]. Platinum or Pt based materials also find relentless application as catalysts in proton exchange membrane fuel cells for both anodic and cathodic electrochemical reactions [13, 14]. The improved electron mobility and effective mass transfer for reactant molecule along with increased active surface area make Pt / Pt based nanostructures an effective electrocatalyst for both oxygen reduction reaction (ORR) and methanol electro-oxidation (MO) [15,16]. Moreover, Pt being a precious metal, nanostructuring strategies leading to reduced usage of Pt mass, while maintaining or enhancing the electrode activity and stability is a field of intense research [17].

Extensive studies have been carried out to investigate the effect of the particle size of Pt [18,19], the structure or arrangement of its atom on the surface [20,21], influence of surface orientation of Pt single crystal [22] and effect of shape on the electrocatalytic activity of Pt [23]. Thus, by tailoring the surface properties of Pt nanoparticles suitably, it is possible to tune them for a specific application. Several attempts have been made with the view to synthesizing Pt nanoparticles with desired properties in order to achieve maximum electrocatalytic activity [9,13,21].

For electrode applications, it is necessary to coat Pt nanoparticles over suitable supporting materials [24, 25]. Efficiency of electrochemical processes like electro-reduction of nitric acid, electro-reduction of oxygen in acidic medium and electro-oxidation of methanol etc., depend on the distribution, preparation methods, and adhesion along with the interaction between nanoparticles and substrates. Though carbon based materials are widely accepted as support materials, they have drawbacks like the loss of catalytic activity, poor surface stability and intermediate poisoning associated with them [26]. Thus, designing a non carbon support material with high specific surface area and stability can improve the performance to a greater extent. Recently, metallic substrate like Ti was used as support material for Pt loading and was found to be effective for alcohol electro-oxidation [27]. A number of strategies have been evolved for developing high performance supporting materials for loading Pt, which include depositing Pt on oxides [28], synthesizing ultra-thin Pt, Pd and alloy nano wires [29] graphene [30] etc. The thermal stability, corrosion resistance and non-toxicity make TiO_2 nanotube (TiNT) a better supporting material. Several studies were carried out by loading metal nano particles like Pt, Pd, Ru etc. on TiNT powders and casting them on other substrates in order to achieve enhanced catalytic activity [31-33]. Vertically aligned TiNT provides larger specific area resulting in

Corrosion Science and Technology Group,Indira Gandhi Centre for Atomic Research, Kalpakkam 603102, India ***Corresponding author**: Email: kamachi@igcar.gov.in, ukmudali@gmail.com, Tel: + 91-4427480121, Fax: + 91-4427480121*
Postal address: Associate Director, CSTG,Indira Gandhi Centre for Atomic Research, Kalpakkam – 603102, India

more dispersed Pt nanoparticles and can serve as a better electrode material. Such vertically aligned nanotubes of Ti can be easily fabricated by simple electrochemical anodization of planar Ti [34, 35]. Zhao et al. [36] discussed in detail the role of vertically aligned TiNT as support material for electrocatalytic application. They reported that nanotubular metallic support provides favorable physicochemical stability and avoids catalyst loss and poisoning. The large surface area of TiNT substrate considerably increased the stability, catalytic efficiency and life time of the cell. Moreover, the hollow and open structure of nanotube array could considerably improve the mass transport and catalyst utilization with minimum dissolution, Ostwald ripening and aggregation throughout the fuel cell operation [37]. To synthesize Pt nanoparticle electrode with TiNT array support, several methods have been adopted [36,38,39]. The major drawback in most of the methods other than sputter coating is the aggregation of Pt particle resulting in reduced catalytic activity [36, 40]. Wet impregnation is the most widely used method for synthesizing supported Pt catalyst [41, 42]. Generally in an impregnation method, the support will be immersed in a solution containing precursor material, which, in subsequent steps will be dried to remove the imbibed solvent. In most of the impregnation methods, additional steps of drying and calcinations are required and the maximum loading is limited by the precursor solubility in the solution. If the Pt nanoparticle can be loaded inside TiNT array, significant improvement in particle dispersion resulting in excellent electrocatalytic activity can be achieved due to the availability of larger surface area. However, it is still considered as a big challenge to load Pt nanoparticle inside the vertically aligned nanotube arrays because of the difficulties involved in controlling the nucleation and growth of the nanoparticle when the reduction kinetics varies for different precursors [37].

One of the major problems associated with Pt catalyst in fuel cell application is the poisoning of its surface by carbon monoxide. Due to CO poisoning, the Pt catalyst will be deactivated in the electro-oxidation of methanol which will hinders its technological viability [43]. It is reported that, the use of TiO_2 or composited TiO_2 hybrid as catalyst could improve the catalytic activity of Pt via bifunctional mechanism [44,45]. A well-defined and aligned TiNT arrays support for Pt catalyst provides superior catalytic activity owing to the fact that the ordered structure of TiNT offers a unidirectional electronic channel and reduces the grain boundaries [33,46].

A novel, effective and highly reproducible seed mediated synthesis method has been developed in the present study for loading Pt nanoparticles on TiNT array support material by hydrothermal reduction. The electrocatalytic capability of nano Pt loaded TiNT was assessed by estimating electrocatalytic active surface area and comparing the result with those of Pt nanoparticle coated Ti support and agglomerated Pt particles on TiNT support material. The superior electrocatalytic activity of Pt loaded TiNT support was demonstrated by measuring the current density in the cyclic voltammogram for methanol oxidation using the three anodes in order to visualize the effect of uniform distribution of Pt nanoparticle and effect of substrate on electrocatalytic activity. The synergistic effect of Pt nanoparticle and TiNT support in enhancing the electrocatalytic activity of nano Pt loaded TiNT electrode has been discussed

Experimental

Synthesis of TiNT array support

A self aligned array of TiNT support material was prepared by electrochemical anodization of Ti metal foil with platinum foil cathode. Commercially pure Ti metal foil (20 x 15 x 0.5 mm), mechanically polished and degreased by sonicating in ethanol and acetone followed by thorough washing in distilled water, was anodized in aqueous ethylene glycol and 0.5% NH_4F in the ratio 3:1. A distance of 1.5 cm was maintained between the electrodes. Potentiostatic anodization was conducted for 1 h at 30 V. The anodized substrates were washed with Millipore water (Milli-Q plus 185 purification system; resistivity: ≥15 MΩ.cm). Further, the TiNT substrates were annealed at 450°C for 3 h to retain crystallinity and to completely eliminate fluoride ions which could have been incorporated inside the nanotube during anodization [47].

Synthesis of Pt nanoparticle loaded TiNT electrode

Electrodeposition of Pt nanoparticle seed. High purity analytical reagent grade chloroplatinic acid (H_2PtCl_6; Pt:40%), sulphuric acid (98%), hydrofluoric acid (40%), hydrochloric acid (35%) and formaldehyde (35%) were used for the synthesis of electrodes. Pt nanoparticle seeds were potentiostatically electrodeposited on TiNT array support using the electrolyte 1 mM chloroplatinic acid in 0.5 M H_2SO_4, at the deposition potential of -0.12 V for about 20 s. The reduction potential for electrodeposition was chosen from the cyclic voltammogram recorded using Pt solution in 0.5 M H_2SO_4 as supporting electrolyte and TiNT array substrate as the working electrode.

Hydrothermal reduction of Pt nanoparticle seeded TiNT array support. Pt nano particles loaded TiNT array support was synthesized via hydrothermal reduction method. The TiNT substrate electrodeposited with Pt seeds was transferred to a Teflon lined stainless steel autoclave. Hydrothermal reduction was carried out in the autoclave for about 10 h at 100°C in a solution of 0.8 g/l chloroplatinic acid and 5 ml of 0.5 % formaldehyde (reducing agent) in Millipore water [48]. For the purpose of comparison, hydrothermal reduction of Pt nanoparticle seeded Ti foil was also carried out under the same condition [49]. After cooling to the room temperature, the coated electrode was washed thoroughly in millipore water and dried in air. During hydrothermal reduction, the temperature can be elevated above the boiling point of water to reach the saturated vapor pressure. The temperature and the amount of solution added to the autoclave largely determine the internal pressure produced.

Surface characterization. The surface morphology of coated electrodes and TiNT array support were analyzed using Field Emission Scanning Electron Microscopy (FESEM) (Hitachi Model - SU6600, Japan). Elemental composition of each electrode was

determined using Energy-dispersive X-ray Spectroscopy (EDS) coupled with FESEM (Horiba, Japan). Phase analysis and structural characterization were carried out using XRD (Rigaku, Japan with Cu Kα radiation) technique. Phase identification and assignment of peaks in XRD pattern were carried out by comparing the peak positions and intensities with the database provided by International Centre for Diffraction Data (ICDD). XPS (SPECS Gmbh (Surface nano Science), Germany) was used for analyzing the oxidation state and surface composition. Monochromatic Al Kα (hu = 1486.7 eV) was used as the source and the internal standard used for binding energy (BE) correction was C 1s peak at 284.8 eV. The amount of Pt loading in each electrode was determined using ICP-OES technique after dissolving each sample in aqua regia.

Electrochemical experiments were carried out at room temperature using an electrochemical workstation, Autolab (PGSTAT-30, Eco-Chemie, the Netherlands) equipped with general purpose electrochemical software. Experiments were conducted in a flat cell, which has a teflon O-ring lined hole on one side allowing only 1 cm^2 area of working electrode to interact with the electrolyte. A Pt foil counter electrode and Ag/AgCl reference electrode were used for the electrochemical experiments. The as synthesized electrodes served as working electrodes. In our earlier study, Pt nanoparticle coated on Ti was extensively studied [49]. The electrochemical behavior of Pt nanoparticle loaded TiNT and agglomerated Pt nanoparticle on TiNT were investigated using cyclic voltammetric technique in acidic medium and compared with that of Pt nanoparticle coated on Ti. For methanol oxidation, pure Ar (99.99%) was bubbled for at least 20 min through the electrolyte, followed by purging over the surface of the solution throughout the measurement to ensure oxygen free solution.

Results and discussion

Morphological and structural characterization of TiNT array. Figure 1 a and b corresponds to the FESEM images and Figs 1 c and d represents the XRD and XPS result of annealed TiNT respectively.

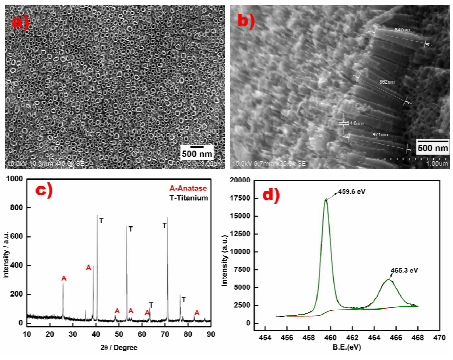

Fig 1. (a) and (b): Top and cross sectional FESEM images of annealed TiNT; (c) and (d): XRD pattern and XPS spectra of annealed TiNT.

Figures 1 a and b reveal that a compact and well ordered TiNT array with an inner diameter of 85 ± 5 nm and a vertical length of approximately 1 µm grew on Ti foil.

The diffraction peaks in Fig. 1 c correspond to anatase TiO_2 crystal structure (tetragonal, JCPDS 89-4921). The peaks with 2θ = 25.6, 38.3 and 48.3 are indexed to (101), (004) and (200) faces of anatase and no specific rutile peak at 2θ = 27 or 31 could be observed [50]. The sharp peaks of Ti are attributed to Ti substrate. The XPS results shown in Fig. 1 d, indicated that Ti $2p_{3/2}$ and Ti $2p_{1/2}$ peaks present at the binding energies 459.6 and 465.3 eV with the peak separation of 5.7 eV are characteristic of Ti^{4+} of TiO_2. The peak symmetry reveals that there was no peak corresponding to Ti^{3+} or Ti^{2+}, which would have been present at 457.6 and 456.4 eV respectively [51]. Additionally, a peak with binding energy of 530.66 eV corresponding to Ti-O bond, as per previous report [52] was observed on analyzing the 1s spectra of O (not shown in Fig. 1 d).

Surface characterization of Pt nano particle loaded TiNT support. Seed mediated reduction method provided a uniform and adherent coating of Pt nanoparticles. Pt seeds with an average size of 150 nm deposited on TiNT by electrodeposition. Hydrothermal reduction of Pt solution with Pt seeded TiNT resulted in uniformly coated surface. Figures 2(a-c) show the FESEM images of (a) Pt nanoparticle loaded TiNT, (b) Pt nanoparticle coated Ti and (c) agglomerated Pt particle coated TiNT. When hydrothermal reduction was done without seeds, Pt particles agglomerated as shown in Fig. 2 c. The seed mediated growth mechanism is a versatile method for efficient dispersion of metal nanoparticle with narrow size distribution, as new nuclei will be favorably deposited over the existing nuclei [53,54].

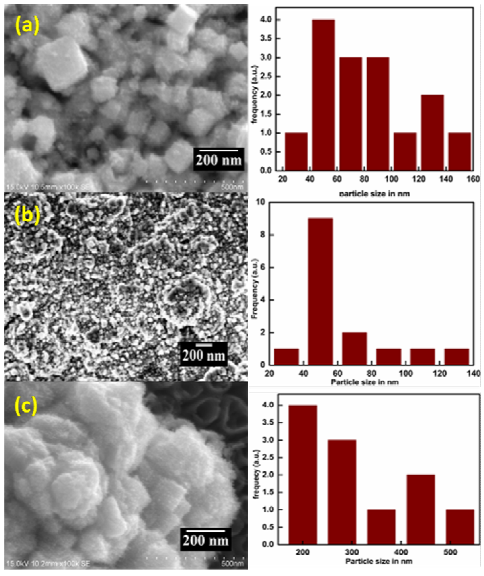

Fig 2. FESEM images of (a) Pt nanoparticle loaded TiNT, (b) Pt nanoparticle coated Ti (c) agglomerated Pt particle coated TiNT and their respective histograms showing particle size distribution.

Pt seeds which were pre-electrodeposited, acted as nucleation sites and enhanced the uniform coverage during hydrothermal reduction. It could also be observed from Fig. 2a that seed mediated hydrothermal reduction resulted in the formation of some cubic Pt nanoparticles with size ranging from 46 to 200 nm. Figure 2 b corresponds to an uniformly distributed Pt nanoparticle coated Ti support synthesized via seed mediated hydrothermal reduction method [49].

To confirm the loading of Pt nano particles inside TiNT, the cross sectional FESEM image was taken. Figure 3 shows FESEM image and corresponding EDS spectrum of the top cross sectional view of Pt loaded TiNT. Inset shows the cross sectional view of the walls of TiNT. It is evident from this figure that Pt particles were loaded on the surface as well as inside the TiNT arrays.

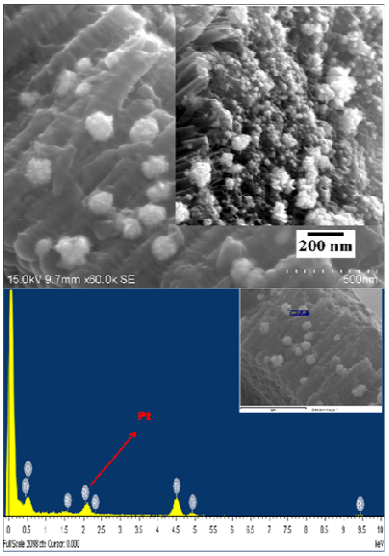

Fig 3. FESEM and EDS spectrum of the top cross sectional view of Pt loaded TiNT. Inset shows the cross sectional view of the walls of TiNT

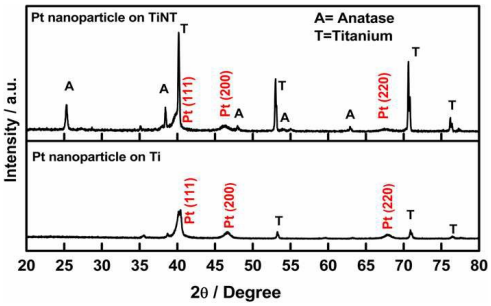

Fig 4. XRD patterns of Pt nanoparticle coated Ti and Pt nanoparticle loaded TiNT

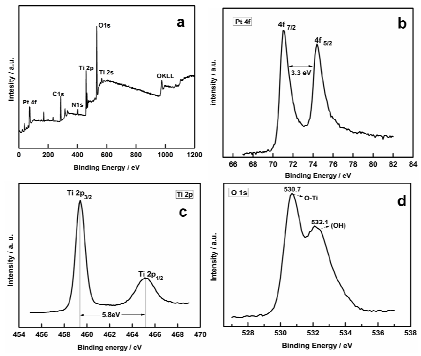

Fig 5. XPS spectra of (a) survey spectrum, (b) Pt 4f, (c) Ti 2p and (d) O 1s of Pt nanoparticle loaded TiNT

The XRD pattern of Pt nanoparticle loaded TiNT and Pt nanoparticle coated Ti are shown in Fig. 4. It was observed that Pt nano particles in both electrodes have (111), (200) and (220) diffraction peaks which are characteristics of face centered cubic (fcc) crystal structure (JCPDS 04-0802). Peaks corresponding to anatase TiO_2 and metallic Ti present in the figure are the characteristic peaks of support material. It is evident from this figure that the peaks corresponding to Pt were much broader than that of support material indicating the smaller size of Pt nanoparticle.

The electronic states of Pt, Ti and O of as-synthesized Pt nanoparticle loaded TiNT electrode were comprehensively studied using XPS. Figure 5 shows the corresponding survey spectra of Pt 4f, Ti 2p and O 1s in Pt nanoparticle loaded TiNT array support. Two distinct peaks at the binding energies 71.1 and 74.4 eV in the Pt 4f core level spectra (Fig. 5 b) could be attributed to Pt $4f_{7/2}$ and $4f_{5/2}$ with a spin orbit splitting of 3.3 eV, thereby confirming the presence of metallic Pt [55, 56]. Peaks corresponding to other oxidation states of Pt could not be observed. The peak at 530.7eV of O 1s spectra represents the lattice O bonded with Ti of TiO_2 and a peak at 532.1 eV corresponds to surface contaminants or surface hydroxides [52].

Though Pt was present as metallic form in Pt nanoparticle loaded TiNT, the spectra of Pt $4f_{7/2}$ and $4f_{5/2}$ showed a shift to lower binding energies with respect to Pt nanoparticle coated Ti by 0.2 eV. Figure 6 shows the comparative spectra (Pt 4f core level) of Pt nanoparticle coated TiNT and Pt nanoparticle coated Ti. This result indicates the possible electronic interaction between Pt and the support material [57, 58]. The observations by Antolini [58] that there could be a possible electronic transfer or charge transfer between Pt and TiO_2 support, corroborate the present result. Such an interaction will result in core level binding energy shift of Ti 2p peak to a higher value in TiO_2 NT spectra. Thus, Ti 2p signal of Pt loaded TiNT was investigated in detail and compared with that of bare TiO_2. It is evident from Fig 7 that the binding energy value of Ti $2p_{3/2}$ was shifted to negative value when TiO_2 acted as Pt nanoparticle support.

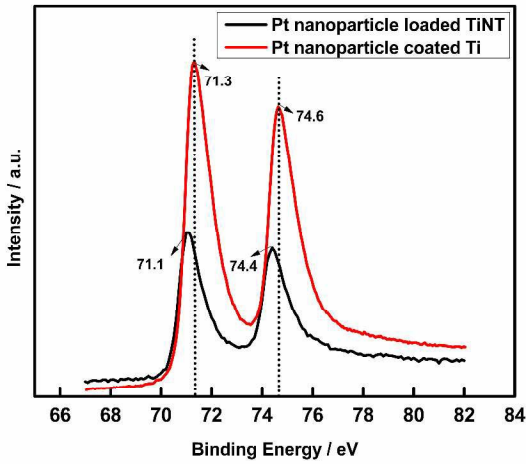

Fig 6. Pt 4f core level XPS spectra of Pt nanoparticle coated TiNT and Ti

The $2p_{3/2}$ signal for bare TiO_2 was observed at 459.60 eV whereas, Pt loaded sample had binding energy value of Ti $2p_{3/2}$ at 459.40 eV. These values are in accordance with that reported for TiO_2 in literature [52]. Taking into account of the direction of shift in binding energy for Pt 4f and Ti 2p of Pt nanoparticle loaded TiNT, electron donation by Ti is not possible. Similar behaviour of shift in binding energy of Pt 4f and Ti 2p in $Pt/TiO_2/C$ was reported by Lewera et al. [59]. They ascribed the possibility of an alloy formation between Pt and TiO_2, which had resulted in lattice strain and creating shift in binding energy. A possible charge transfer could also have occurred, since the peak width and peak symmetry of Pt varied (Figure 6) in Pt nanoparticle loaded TiNT, indicating an increased electron density on Pt [60]. The binding energy shift towards lower value was observed by Chen et al. [61] for both Pt 4f and Ti 2p, when Pt was deposited on TiO_2 and they suggested a possible enhancement in catalytic activity with respect to the degree of electron donation from support to the metal.

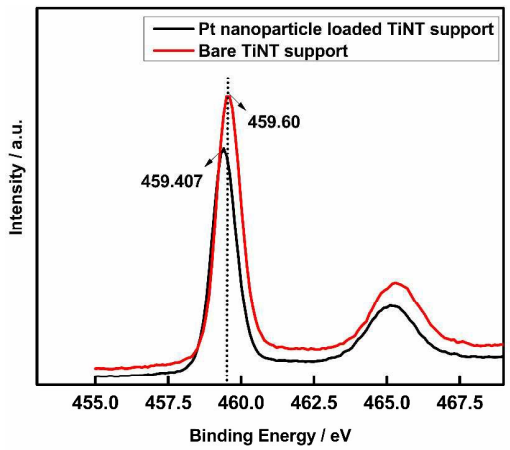

Fig 7. XPS spectra of Ti 2p for TiNT and Pt nanoparticle loaded TiNT

Thus, it is concluded that, the TiNT array support has a prominent role on the electrocatalytic activity of Pt nanoparticle deposited on it.

Electrocatalytic activity of synthesized electrodes. To estimate the electrocatalytic activity of the developed electrodes, cyclic voltammograms of Pt nanoparticle loaded TiNT, agglomerated Pt nanoparticle deposited TiNT and Pt nanoparticle coated Ti were recorded in 1 M H_2SO_4 under inert atmosphere and the results recorded after 5 cycles are presented in figure 8. The typical cyclic voltammograms (CV) showed regions corresponding to Pt-O formation, reduction of oxide layer and peaks for hydrogen adsorption –desorption on Pt surface. This confirmed that good electronic contact was existing between the Pt nanoparticles and both TiNT and Ti support material. For an electrocatalyst, the electrochemically active surface area (ECSA) is an important parameter, as it determines the electrocatalytic capability. The ECSA of a Pt electrode could be calculated from the hydrogen adsorption/desorption peak, as the integrated intensity of the peaks represent the available Pt sites. Thus, the charge obtained from hydrogen adsorption/desorption region (Q_H), after eliminating the charge corresponding to double layer was used to calculate the ECSA using the following equation (1) [62,63]:

$$Pt_{ECSA} = Q_H / (Q_{ref} \times Pt\ loading) \quad (1)$$

where Q_{ref} = 0.21 mC/cm^2 (the charge required for monolayer hydrogen adsorption on smooth polycrystalline Pt surface) [64].

Atomic absorption spectroscopic analysis yielded the Pt loading values as 0.51, 0.48 and 0.42 mg/cm^2 for Pt nanoparticle loaded TiNT, agglomerated Pt nanoparticle coated TiNT and Pt nanoparticle coated Ti respectively. The Q_H value calculated for three electrodes by integrating the respective electro-adsorption curve for hydrogen after subtracting double layer region and dividing by scan rate were found to be 22.804, 8. 22.69 mC/cm^2 respectively. From the Q_H value, the amount of Pt loading can be calculated using the equation (1) and the values are 212.923, 88.94 and. 257.25 cm^2/mg. The ECSA was found to be more for Pt nanoparticle coated Ti than Pt nanoparticle loaded TiNT because more number of Pt nanoparticles are present on the surface than Pt nanoparticle loaded TiNT.

Methanol electro oxidation reaction. The electrochemical methanol oxidation behaviour of the electrodes were investigated by conducting cyclic voltammetry in 0.1 M CH_3OH+0.5 M H_2SO_4 solution. Figure 9 represents the mass normalized voltammetric behaviour of (20th cycle) Pt nanoparticle loaded TiNT, Pt nanoparticle loaded Ti, and agglomerated Pt particle coated TiNT. No significant methanol oxidation peak was observed for TiNT electrode for methanol electro-oxidation. For the Pt coated electrodes two anodic peaks were observed in the voltammogram. The anodic peak observed during forward scan between 0.2 V and 0.9 V corresponds to electro-oxidation of methanol, and the peak appeared during the reverse scan between 0.5 V and 0.1 V

corresponds to the removal of incompletely oxidized residual carbon species generated during forward scan on the surface [65, 66]. A broad and less intense anodic peak appeared at about 1.1 V in the CV of nano Pt coated TiNT and Ti substrates is also attributed to the methanol oxidation, probably due to change in oxide structure. According to Seland et al. [67] the adsorbed CO will be oxidized by the oxide formed and the clean surface facilitates further oxidation of methanol.

The methanol oxidation activity for agglomerated Pt particle on TiNT was considerably lower than both Pt nanoparticle loaded TiNT and Pt nanoparticle coated Ti, which could be due to the increased size of Pt particle resulting in reduced catalytic activity. It could also be noted that though the ECSA of Pt nanoparticle coated Ti and Pt nanoparticle loaded TiNT are comparable, the increment in current density for mass normalized methanol oxidation was much higher for Pt nanoparticle loaded TiNT than Pt nanoparticle coated Ti.

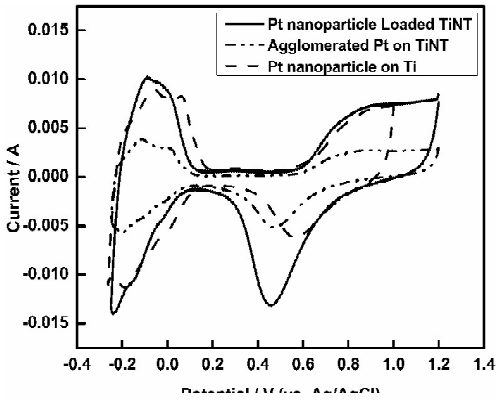

Fig 8. Cyclic Voltammograms of Pt nanoparticle loaded TiNT, agglomerated Pt particle on TiNT and Pt nanoparticle coated Ti in 1 M H_2SO_4

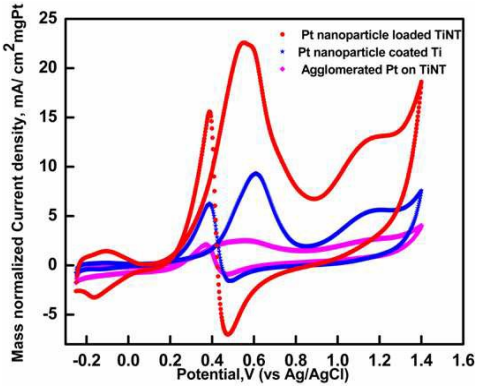

Fig 9. Cyclic voltammograms of Pt nanoparticle loaded TiNT, Pt nanoparticle loaded Ti, agglomerated Pt particle coated TiNT in 0.1M CH_3OH+0.5M H_2SO_4 solution

The catalytic activity of nano Pt loaded TiNT was also found to be much higher (current density (CD): 11.75 mA/cm^2) than that for a commercial Pt coated Ti anode (CD: 0.05 mA/cm^2) in methanol oxidation experiment under identical conditions. This excellent activity of Pt nanoparticle loaded TiNT for methanol oxidation confirms that, the support TiNT has a definite role in enhancing the electrocatalytic activity of Pt. According to Chen et al. [44] this electrocatalytic activity enhancement could be due to a synergistic effect of Pt nanoparticle and TiO_2 support. They also suggested that TiO_2 interacts via a bifunctional mechanism wherein, it promotes oxidation and removal of adsorbed CO from Pt catalyst surface as well as modifies electronic structure of Pt nanoparticle by means of electronic effect.

Supported Pt or modified Pt catalysts were found to have enhanced electrocatalytic activity due to bifunctional mechanism. That is, combining each individual element in a synergistic fashion generating a surface with improved catalytic activity than individual elements [44,68,69]. Thus by modifying the nature of Pt surface, the oxygen containing species will be adsorbed at lower overpotentials than pure Pt surface which will in turn initiate the electro-oxidation of CO adsorbed on nearby Pt sites. Moreover, the anatase TiNT support of Pt nanoparticle can generate OH_{ad} species during electrochemical processes, which can assist in removing CO like intermediates via oxidizing them, thereby reducing the poisoning of Pt catalyst [44, 69].

The dissociative adsorption of water molecule on TiNT surface could result in the formation of Ti-OH surface group, which can potentially oxidize the CO_{ad} on the periphery of Pt nanoparticles via a bifunctional mechanism. As the immediate contact of CO_{ad} with Ti-OH group occurs at the periphery, the electrooxidation of CO occurs predominantly at the periphery region of Pt nanoparticle. As more and more free Pt sites are available, the rate of CO oxidation also increases. Additionally, TiNT can also modify the electronic structure of Pt nanoparticles in terms of electronic effect. Interaction with TiNT support influence or alter the properties of the chemisorbed noble metal particle [70].

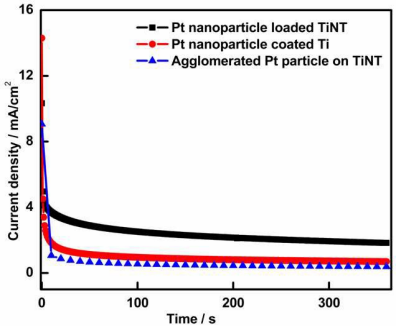

Fig 10. Chronoamperogram of Pt nanoparticle loaded TiNT, Pt nanoparticle loaded Ti, agglomerated Pt particle coated TiNT in 0.1M CH_3OH+0.5M H_2SO_4 solution

The strong d electron interaction between TiNT support and Pt nanoparticle can influence the electronic structure of Pt atoms at the interface resulting in improved catalytic activity. This modification of electronic structure of Pt can alter the adsorption strength of CO_{ad} species, reducing the activation barrier for electrochemical oxidation reaction. The XPS results (Figure 6 and 7), clearly indicated the effect of substrate on the Pt particle. The electronic effect was more pronounced on peripheral Pt atoms which are in direct contact with the TiO_2 support and therefore, exhibits distinct electrocatalytic activity than surface atoms. Thus the synergistic effect of Pt nanoparticle and TiNT support has enhanced the electrocatalytic activity of Pt loaded TiNT than the Pt coated Ti and agglomerated Pt coated TiNT. Li et al. [71] reported that, compared to Pt nano particle on flat Ti surface, Pt nanoparticle on TiNT provided better contact area between Pt and metal substrate resulting in superior catalytic activity and stability. The FESEM cross sectional image (Figure 3) revealed that, Pt nanoparticles were also loaded inside and on the walls of TiNT resulting in increased conductivity.

The electrocatalytic activity of the three electrodes was further evaluated by recording chronoamperograms at a fixed potential in 0.1 M CH_3OH +0.5 M H_2SO_4 solution. The potential of the electrodes were maintained at 0.60 V and the current flowing through the electrode was monitored for 360 s. The high current observed initially in Fig 10 originates from double layer charging. A steady state was attained after the sharp decay of initial current. The decay rate constants for three electrodes, Pt nanoparticle loaded TiNT, Pt nanoparticle coated Ti and agglomerated Pt particle coated TiNT were calculated to be 0.05, 0.15 and 0.18 /s respectively. A slow decay of current was observed for Pt nanoparticle loaded TiNT compared to the other two electrodes, indicating better catalytic stability and tolerance to poisonous CO like intermediate. The current density value was also found to be higher for Pt nanoparticle loaded TiNT than Pt nanoparticle coated Ti and agglomerated Pt particle coated TiNT. The chronoamperometric results confirmed that Pt nanoparticle loaded on TiNT substrate has a better electrocatalytic activity than Pt nanoparticle coated on Ti substrate, and thus implying that TiNT substrate exhibits a prominent role in enhancing the electrocatalytic activity of Pt nanoparticle coated on it.

Conclusions

Titanium substrate was nanostructured to TiNT via electrochemical anodization. Pt seeds were electrodeposited on TiNT and subsequently Pt nanoparticles were uniformly coated on TiNT substrate via hydrothermal reduction. The absence of Pt seeds resulted in agglomerated Pt particle coating on TiNT during hydrothermal reduction. The FESEM results indicated that the Pt nanoparticles were present both inside and outside the TiNT. The electronic interaction between the Pt nanoparticle and TiNT was established by XPS analysis by comparing the peak position of Pt nanoparticle on Ti substrate and Pt nanoparticle coated on TiNT substrate. The electrochemically active surface area of Pt nanoparticle loaded TiNT and Pt nanoparticle coated Ti were comparable and it was higher than that of agglomerated Pt particle coated TiNT. Though, ECSA was found to be comparable, the electrocatalytic activity of Pt nanoparticle loaded TiNT was far superior than Pt nanoparticle coated Ti suggesting that substrate has a definite role in enhancing the electrocatalytic activity of Pt nanoparticle coated on it.

Acknowledgements

Authors would like to acknowledge National Centre for Nanoscience and Nanotechnology, University of Madras, Guindy Campus and its Director Dr. S. Balakumar for FE- SEM characterization and Mr. Nanda Gopala Krishna, Scientific Officer D (Corrosion Science and Technology Group) for XPS characterization.

References

1. M. Dekkar *Metal nanoparticles Synthesis, Characterization and Applications*, (Eds: D.L. Feldheim, C. A. Foss, Jr), New York 2002.
2. B. L. Cushing, V. L. Kolesnicheniko, C. J. O' Connor, *Chem. Rev.,* 2004, **104**, 3893
3. E. Ramirez, L. Eradès, K. Philippot, P. Lecante, B. Chaudret, *Adv. Funct. Mater.*,2007, **17**,2219
4. K. Koczkur, Q. Yi, A. Chen, *Adv. Mater.*, 2007, **19**, 2648
5. S. J. Cho, J. Ouyang, *J Phys Chem C,* 2011,**115**,8519
6. C. Mallika, B. Keerthika, U. Kamachi mudali, *Electrochimica Acta,* 2007, **52**, 6656
7. U. Kamachi mudali, V. R. Raju, R.K. Dayal, *J. Nucl. Mater*., 2000, **277** 49.
8. B. O'Regan, M. Grätzel, *Nature,* 1991**353**, 737.
9. H. Boo, S. Park, B. Ku, Y. Kim, J. H. Park, H. C. Kim, T. D. Chung *J. Am. Chem. Soc.,* 2004 **126** 4524
10. J Xie, S Wang, L Aryasomayajula, V K Varadan *Nanotechnology*, 2007, **18,** 65503.
11. H. F. Cui, J. S. Ye, X. Liu, W. D. Zhang, F. S. Sheu, *Nanotechnology*, 2006, **17**, 2334.
12. K. Sun, B. Fan, J. Ouyang, *J. Phys. Chem. C*, 2010, **114** (9), 4237.
13. S. A. Lee, K.-W. Park, J. H. Choi, B. K. Kwon, Y. E. Sung, *J. Electrochem. Soc.*, 2002, **149**, A1299
14. Y. Mu , H. Liang , J. Hu , L. Jiang, L. Wan, *J. Phys. Chem. B*, 2005, **109,** 22212..
15. E. Antolini, R.C. Jose, E.R. Salgado, Gonzalez, *Appl. Catal. B*: *Environ.*, 2006, **63,**137.
16. Q. Yi, L. li, W. Yu, Z. Zhou, X. Liu, G. Xu, *J. Alloy Compd*, 2008, **466,** 52.
17. A. Kloke, F. V. Stetten, R. Zengerle , S. Kerzenmacher, *Adv. Mater.,* 2011, **23,** 4976.
18. R. Narayanan, M. A. El-Sayed, *J. Phys. Chem. B*, 2005, **109**, 12663.

19. M. Shao, A. Peles, K. Shoemaker, *Nano Lett.,* 2011, **11 (9),** 3714.
20. S. Cheong, J. D. Watt, R. D. Tilley, *Nanoscale*, 2010, **2**, 2045
21. D. Dixon, J. Melke, M. Botros, J. Rathore, H. Ehrenberg, C. Roth, *Int J Hydrogen Energ*, 2013, **38,** 13393.
22. C. Wang, H. Daimon, Y. Lee, J. Kim, S. Sun, *J. Am. Chem. Soc*., 2007, **129**, 6974.
23. S. Kinge, C. Urgeghe, A. De Battisti, H. Bönnemann, *Appl. Organomet. Chem,* 2008, **22**, 49.
24. B. Singh,E. Dempsey, *RSC Adv.*, 2013, **3**, 2279
25. L. Jiang, H. Fu, L. Wang, W. Zhou, B. Jiang, R. Wang, *RSC Adv*.,2014,**4**,51272
26. C.C yang, S. J. Chiu, w. C. Chien, *J power sources,* 2006, **162**,21.
27. J. Lu, S. Lu, D. Wang, M. Yang, Z. Liu, C. Xu, S. P. Jiang, *Electrochim. Acta*, 2009, **54,** 5486.
28. Y. Li, Y Li, E. Zhu, T. McLouth, C.-Y Chiu, X. Huang, Y. Huang, J. Am. Chem. Soc., 2012, 134, 12326]
29. C. Koenigsmann, W. Zhou, R. R. Adzic, E. Sutter, S. S. Wong, Nano Lett., 2010, 10, 2806]
30. Y. Q. Sun, Q. Wu, G. Q. Shi, Energy Environ. Sci. 2011, 4, 1113]
31. F. Hu, F. Ding, S. Song, P. K. Shen*, J. Power Sources,* 2006, **163,** 415.
32. S. Beak, D. Jung, K. S. Nahm, P. Kim, *Catal. Lett*., 2010, **134,** 288.
33. C. Zhai, M. Zhu, D. Bin, H. Wang, Y. Du, C. Wang, P Yang, ACS applied materials & interfaces, 2014, 6 (20), 17753].
34. C. Ruan, M. Paulose, O. K. Varghese, G. K. Mor, C. A. Grimes, *J. Phys. Chem. B*, 2005, **109**, 15754.
35. D. Gong, C. A Grimes, O. K. Varghese, W. Hu, R. S. Singh, Z. Chen, E. C Dickey, J. Mater. Res., 2001, **16,** 3331.
36. Y. Lei, G. Zhao, X. Tong, M. Liu, D. Li, R. Geng, *ChemPhysChem* 2010, **11**, 276.
37. A.L Wang, H. Xu, J. X. Feng, L. X. Ding, Y. X. Tong, Gao-Ren Li, J. Am. Chem. Soc., 2013, **135 (29)**, 10703
38. M.B. Hassan, H. Nanjo, S. Venkatachalam, M. Kanakubo, T. Ebina, *J. Power Sources,* 2010, **195,** 5889.
39. L. Yang, W. Yang, Q. Cai*, J. Phys. Chem. C*, 2007, **111,** 16613.
40. Y. Y. Song, Z. D. Gao, P. Schmuki, *Electrochem.Commun*., 2011 **13,** 290.
41. L. Wang, Q. Zhang, M. Sakurai, H. Kameyama, Catal. Commun. 2007, **8**, 2171;
42. D. Feng, Z. Rui, Y. Lu, H. Ji, Chemical Engineering Journal, 2012**, 179**, 363.
43. S, Wasmus, A. Kuver, J. Electroanal. Chem., 1999, 461, 14; Z. Jusys, H. Massong and H. Baltruschat, J. Electrochem. Soc.,1999, **146**, 1093
44. C. S. Chen, F. M. Pan, Appl. Catal. B: Environ., 2009, **91**, 663.
45. S, Wasmus, A. Kuver, J. Electroanal. Chem., 1999, **461**, 14
46. L. Xing, J. Jia, Y. Wang, B. Zhang, S. Dong, Int. J. Hydrogen Energy 2010, **35**, 12169
47. W. J. Lee, M. Alhoshan, W. H. Smyrl, *J. Electrochem. Soc.*, 2006, **153,** B499.
48. K. R. Rasmi, S. C. Vanithakumari, R. P. George and U. K. Mudali, *J. Mater. Eng. Perform.,* 2014, **23,** 1673
49. K. R. Rasmi, S. C. Vanithakumari, R. P. George, C. Mallika, U. K. Mudali, *Mat Chem. Phys,.* 2015, **151,** 133
50. L. Gu, J. Wang, H. Cheng, Y. Du, X. Han, *Chem. Commun.,* 2012, **48,** 6978.
51. D. Chu, A. Younis, S. Li, *J. Phys. D: Appl. Phys.,* 2012, **45,** 355306
52. R. P. Antony, T. Mathews, S. Dash, A. K. Tyagi, B. Raj, *Mat Chem. Phys.,* 2012, **132**, 957.
53. T. Liu, D. Li, D. Yang, M. Jiang, *Colloids Surf A Physicochem Eng Asp*., 2011, **387,** 17.
54. G. Chang, M. Oyama, K. Hirao, *J. Phys. Chem. B,* 2006, **110,** 20362.
55. F. C. Wang, C. H. Liu, C. W. Liu, J. H. Chao, Ch. H. Lin, J. *Phys. Chem. C*, 2009, **113,** 13832.
56. Z. Ozturk, F. Sen, S. Sen, G. Gokagac, *J Mater Sci,* 2012, **47,** 8134.
57. Z. Awaludin, M. Suzuki, J. Masud, T. Okajima, T. Ohsaka, *J. Phys. Chem. C,* 2011, **115,** 25557.
58. E. Antolini, J. Mater. Sci., 2003, **38,** 2995.
59. L. Timperman, A. Lewera, W. Vogel, N. Alonso-Vante , Electrochem. Commun., 2010, **12,** 1772.
60. A. Lewera, L. Timperman, A. Roguska, N. Alonso-Vante, J. *Phys. Chem. C*, 2011, **115,** 20153.
61. B. H. Chen, J. M. White, *J. Phys. Chem*. 1982, **86,** 3534.
62. B. Abida, L. Chirchi, S. Baranton, T. W. Napporn, H. Kochkar, J. M. Léger, A. Ghorbel, *Appl. Catal. B*: *Environ.*, 2011, **106,** 609
63. S. H. Sun, D. Q. Yang, D. Villers, G. X. Zhang, E. Sacher, J. P. Dodelet, *Adv.Mater*., 2008, **20,** 571
64. J. M. D. Rodríguez, J. A. H. Melián, J. P. P., *J ChemEd.chem.wisc.edu.,* 2000, **77**, 1195.
65. L. Xing, J. Jia, Y. Wang, B. Zhang, S. Dong, *Int J Hydrogen Energ*, 2010, **35,** 12169.
66. X. Huang, Z. Li, X. Zhang, X. He, S. Lin, *J Colloid Interf Sci.,* 2013, **393,** 300.
67. F**.** Seland, R**.** Tunold, D**.** A. Harrington, Electrochim Acta, 2006, **51 (18),** 3827
68. Z. Jusys, H. Massong and H. Baltruschat, J. Electrochem. Soc.,1999, **146,** 1093]
69. E. Formo, Z. Peng, E. Lee, X. Lu, H. Yang, Y. Xia, J. Phys. Chem. C, 2008, **112 (27),** 9970.
70. J.R. Croy, S. Mostafa, J. Liu, Y. Sohn, H. Heinrich, B.R. Cuenya, Catal. Lett., 2007, **119,** 209.
71. H. Li, J. Wang, M. Liu, H. Wang, P. Su, J. Wu, J. Li, *Nano Research*, 2014, **7**, 1007.